

See discussions, stats, and author profiles for this publication at: <https://www.researchgate.net/publication/5328885>

# Supramolecular Self-Assembly of Amphiphiles on Carbon Nanotubes: A Versatile Strategy for the Construction of CNT/Metal Nanohybrids, Application to Electrocatalysis

ARTICLE in JOURNAL OF THE AMERICAN CHEMICAL SOCIETY · AUGUST 2008

Impact Factor: 12.11 · DOI: 10.1021/ja8026373 · Source: PubMed

CITATIONS

90

READS

51

9 AUTHORS, INCLUDING:



Hynd Remita

Université Paris-Sud 11

113 PUBLICATIONS 2,169 CITATIONS

SEE PROFILE



Bineta Keita

Université Paris-Sud 11

280 PUBLICATIONS 8,363 CITATIONS

SEE PROFILE



Guangjin Zhang

Chinese Academy of Sciences

73 PUBLICATIONS 1,559 CITATIONS

SEE PROFILE



Eric Doris

Atomic Energy and Alternative Energies Co...

142 PUBLICATIONS 1,673 CITATIONS

SEE PROFILE

## Supramolecular Self-Assembly of Amphiphiles on Carbon Nanotubes: A Versatile Strategy for the Construction of CNT/Metal Nanohybrids, Application to Electrocatalysis

Nicolas Mackiewicz,<sup>§</sup> Geetarani Surendran,<sup>‡</sup> Hynd Remita,<sup>‡</sup> Bineta Keita,<sup>‡</sup> Guangjin Zhang,<sup>‡</sup> Louis Nadjo,<sup>‡</sup> Agnès Hagège,<sup>#</sup> Eric Doris,<sup>\*,§</sup> and Charles Mioskowski<sup>§,†</sup>

CEA, iBiTecS, Service de Chimie Bioorganique et de Marquage, F-91191 Gif sur Yvette, France, Laboratoire de Chimie Physique, Université Paris XI, F-91405 Orsay, France, and Institut Pluridisciplinaire Hubert Curien-DSA, F-67087 Strasbourg, France

Received January 31, 2008; E-mail: eric.doris@cea.fr

Since the discovery of carbon nanotubes (CNTs) by Iijima in 1991,<sup>1</sup> intensive studies of their properties have been carried out, suggesting great potential for applications in nanotechnology. Due to their high specific surface area, electric conductivity, and chemical stability, carbon nanotube nanohybrids are receiving increasing interest for catalytic applications from fuel/electrochemical cells to heterogeneous catalysis. The “bottom-up” construction of such nanodevices requires the assembly of noble metal nanoparticles (NP) on carbon nanotubes, and several routes have been developed to link the metallic particles to their surface.<sup>2</sup> Examples include electroless plating,<sup>3</sup> electrodeposition,<sup>4</sup> chemical deposition,<sup>5</sup> and the direct assembly of NPs.<sup>6</sup> Strategies have also been directed toward the introduction of functional groups on CNTs to create preferred sites for nucleation of metal ions (impregnation process), prior to reduction.<sup>7</sup> These strategies include chemical or electrochemical oxidation at defect sites of carbon nanotubes,<sup>8</sup> wrapping of CNT with polymers,<sup>9</sup> and grafting of tethers such as dendrons.<sup>10</sup>

In this paper, we report an alternative strategy for the anchoring of metallic NP on carbon nanotubes. Our approach is based on the work previously reported by our group on the self-assembly of surfactants and analogous systems on the nanotube surface.<sup>11</sup> This leads to supramolecular structures made of rolled-up half-cylinders orientated perpendicular to the nanotube lattice (Figure 1). When amphiphilic surfactants are mixed with CNT at a concentration greater than the critical micellar concentration (CMC), they self-organize as hemimicelles on the nanotube surface. While the hydrophobic portion of the amphiphile is adsorbed on CNT walls by van der Waals interactions, its hydrophilic headgroup is oriented toward the aqueous phase. This produces half-cylinders that can be visualized by transmission electron microscopy (TEM). Negative staining TEM pictures of coated CNTs showed regular striations on their entire surface. Adsorption of amphiphilic molecules on the nanotubes creates a distribution of ionic species that prevents aggregation and induces stable nanotube suspensions in water. The objective of this study was to take advantage of the high density of potential binding motifs (ionic species) distributed along the nanotube lattice, to anchor and grow the metallic nanoparticles.

Two different amphiphiles were used (Figure 2). Both contained a long alkyl chain for interaction with the nanotube surface and a polar head made of either nitrilotriacetic acid (NTA) or pyridinium, for the binding of the metallic NPs. While the choice of NTA was inspired by the presence of the three chelating carboxylate groups,

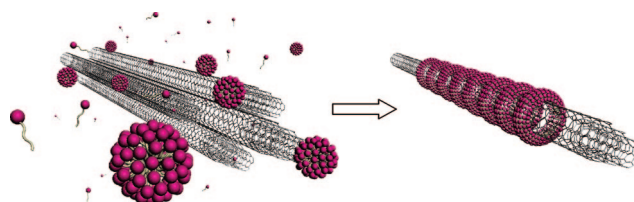


Figure 1. General scheme of amphiphile self-assembly onto CNTs.

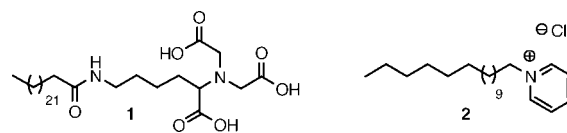


Figure 2. Chemical structure of amphiphiles used in this study.

pyridinium was chosen for its ability to interact through overlapping of its  $\pi$  and  $\pi^*$  orbitals with those of the metal atoms. The synthesis of the NTA-based amphiphile **1** is described in the Supporting Information. The pyridinium-based amphiphile **2** was purchased from a commercial source.

With the above amphiphiles **1** and **2** in hand, we induced their self-assembly on the nanotube surface. In a typical experiment, 10 mg of the surfactant in 2 mL of 100 mM Tris buffer was first sonicated using an ultrasonic tip to stimulate micelle formation. This preliminary step is crucial for efficient assembly of the surfactants on CNTs. Multiwalled carbon nanotubes (MWNTs) (50 mg from *n*-TEC) in 3 mL of the same buffer were sonicated in parallel before being added to the micelle solution. The mixture was further sonicated for 5 min and then centrifuged at 15 000 rpm to remove the excess surfactant molecules. At the end of the process, the nanotubes were dispersed in pure water to reach a final concentration of 0.2 mg/mL (as determined by spectrophotometric absorption). TEM observation of the aqueous dispersions showed, in the two cases studied, the expected self-assembled regular motifs on the graphitic side walls of the nanotubes (Figure 3a,b). The nanotubes fully covered with ionic polar heads were thus exploited, in the following step, for complexation to the metallic NP. The coated carbon nanotubes were subsequently treated with a metal salt. We chose, as model metal, palladium derived from two different complexes:  $\text{Pd}(\text{NH}_3)_4\text{Cl}_2$  or  $\text{Pd}(\text{CH}_3\text{CN})_2\text{Cl}_2$ . The salts were introduced to the reaction mixture to give a final concentration of 0.2 mg/mL. The carbon nanotube/metal salt solution was then allowed to stand for 1 day prior to reduction. This delay provides enough time for the interactions between the coated CNT and the metallic salt to develop. The solutions were deoxygenated under argon for 10 min and the samples submitted to electron beam

<sup>§</sup> CEA, iBiTecS, Service de Chimie Bioorganique et de Marquage.

<sup>‡</sup> Université Paris XI.

<sup>#</sup> Institut Pluridisciplinaire Hubert Curien-DSA.

<sup>†</sup> Deceased June 2, 2007.

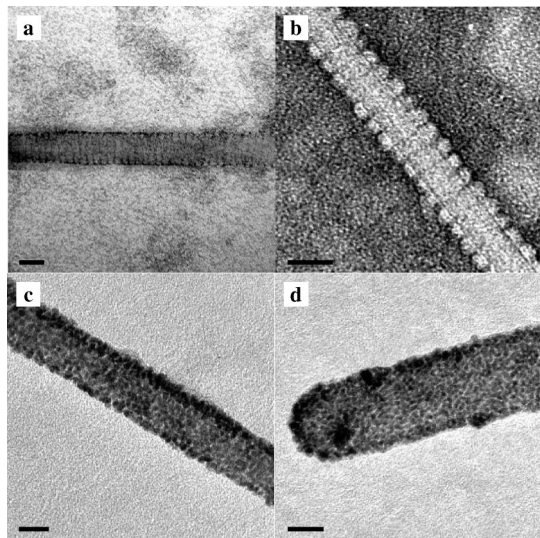


**Figure 3.** TEM pictures CNT functionalized with amphiphile **2** (a) and **1** (b) (negative staining); TEM pictures of Pd nanoparticles on CNT-2 (c) and CNT-1 (d). Scale bar = 20 nm.

irradiation (mean dose rate  $2200 \text{ Gy} \cdot \text{s}^{-1}$ ). Pd salts were reduced in situ by solvated electrons and by radicals originating from solvent radiolysis. Electron beam irradiation has the advantage, over chemical methods, of inducing homogeneous reduction and nucleation which leads to small and monodisperse metal nanoparticles.<sup>12</sup> At the end of the electron beam reduction, the nanotubes were collected by centrifugation, analyzed by TEM, and the metal content was determined by inductively coupled plasma-mass spectrometry (ICP-MS). Similar results were obtained regardless of the palladium complex employed. As shown in Figure 3c,d, TEM pictures confirmed the successful anchoring of the metallic nanoparticles on the CNT side walls. Nanotubes are decorated with a dense and uniform loading of NPs. Their size distribution was evaluated by statistical diameter measurement using selected TEM images. The latter indicated a NP size mainly between 1 and 3 nm with a mean diameter of ca. 2 nm. Noteworthy is that no NP aggregation was observed neither on the nanotube surface nor in solution.

ICP-MS measurements indicated a metal content of 12 wt % for CNTs covered with amphiphile **1** and of 21% for CNTs covered with amphiphile **2**. This technique also permitted the unambiguous characterization of the NP as palladium by isotopic profile comparison; furthermore, selected area diffraction confirmed the metallic nature of Pd (see Supporting Information). Control experiments were run in parallel using the overall same sequence, without initial coating of the nanotubes. At the end of the reduction process, the samples were again analyzed by TEM and ICP-MS. TEM images of pristine nanotubes that were reacted with Pd salts showed sparse nanoparticle distribution. This trend was further confirmed by ICP-MS, which indicated low metal content on carbon nanotubes (4% by mass). This result was anticipated since the control sample was composed of “naked” nanotubes that were not covered with the amphiphilic binding motifs. In addition, the nanotubes have not been oxidatively treated and therefore do not incorporate carboxylic groups which could have served as anchoring moieties for the metallic NP. These experiments demonstrate that the initial self-assembly of the surfactants on the nanotube is a key element for successful metallic nanoparticle deposition. The surfactant coating of the nanotube also strengthens the interaction

between the carbonous template and the metallic NP. While several washings with water induce progressive release of the NPs from the pristine CNT surface, constant NP loading was measured in the case of surfactant-mediated deposition.

With the Pd-coated nanotubes in hand, their performances toward electrocatalytic oxidation of 1 M EtOH in 1 M KOH were evaluated by cyclic voltammetry at a scan rate of  $50 \text{ mV} \cdot \text{s}^{-1}$ . Three different samples were tested: CNT-1-Pd, CNT-2-Pd, and pristine CNT-Pd. The following parameters, including the faradaic onset potential ( $E_{\text{onset}}$ ), the forward peak potential ( $E_f$ ), the backward peak potential ( $E_b$ ), the forward peak current intensity ( $I_f$ ) expressed in  $\text{mA} \cdot \text{cm}^{-2} \cdot \text{mg}^{-1}$  of Pd are shown in Table S1 and the cyclic voltammograms are provided in Figures S4–S6 (see Supporting Information). Among these parameters, the most striking differences appear with respect to current intensities. The large superiority of CNT-1-Pd in terms of current intensity is obvious, being nearly 25 times higher ( $3540 \text{ mA} \cdot \text{cm}^{-2} \cdot \text{mg}^{-1}$ ) than that of previously reported MWCNT-Pd assemblies.<sup>13</sup> The electrodes were also tested for their durability under continuous cycling between  $-1.02$  and  $-0.220 \text{ V}$ . Comparisons were made after 200 cycles. It is remarkable that 94 and  $\sim 100\%$  of the initial current was still observed for CNT-1-Pd and CNT-2-Pd, respectively. These characteristics designate our nanohybrids among the best systems for ethanol oxidation.

In conclusion, we have shown that the hemimicelle self-assembly of amphiphilic molecules provided an effective template for the homogeneous and dense deposition of noble metal nanoparticles on carbon nanotubes. Electrocatalytic applications of the resulting nanohybrids were evaluated, and superior activity in certain oxidation reactions, compared to analogous systems, was observed. Hence, CNT/amphiphile/NP nanohybrids are emerging as promising systems for fuel cell applications.

**Acknowledgment.** Dr. Alexander Yuen is gratefully acknowledged for helpful discussion.

**Supporting Information Available:** Experimental procedures, isotopic profile of Pd, SEAD, Table S1, Figures S4–S6. This material is available free of charge via the Internet at <http://pubs.acs.org>.

## References

- (1) Iijima, S. *Nature* **1991**, *354*, 56.
- (2) Georgakilas, V.; Gournis, D.; Tzitzios, V.; Pasquato, L.; Guldi, D. M.; Prato, M. *J. Mater. Chem.* **2007**, *17*, 2679.
- (3) Qu, L.; Dai, L. *J. Am. Chem. Soc.* **2005**, *127*, 10806.
- (4) Quinn, B. M.; Dekker, C.; Lemay, S. G. *J. Am. Chem. Soc.* **2005**, *127*, 6146.
- (5) Li, W.; Liang, C.; Zhou, W.; Qiu, J.; Zhou, Z.; Sun, G.; Xin, Q. *J. Phys. Chem. B* **2003**, *107*, 6292.
- (6) (a) Han, X.; Li, Y.; Deng, Z. *Adv. Mater.* **2007**, *19*, 1518. (b) Kongkanand, A.; Vinodgopal, K.; Kuwabata, S.; Kamat, P. V. *J. Phys. Chem. B* **2006**, *110*, 16185. (c) Ou, Y. Y.; Huang, M. H. *J. Phys. Chem. B* **2006**, *110*, 2031.
- (7) (a) Waje, M. M.; Wang, X.; Li, W.; Yan, Y. *Nanotechnology* **2005**, *16*, S395. (b) Kim, Y. T.; Ohshima, K.; Higashimine, K.; Uruga, T.; Takata, M.; Suematsu, H.; Mitani, T. *Angew. Chem., Int. Ed.* **2006**, *45*, 407.
- (8) (a) Li, J.; Tang, S.; Lu, L.; Zeng, H. C. *J. Am. Chem. Soc.* **2007**, *129*, 9401. (b) Kim, D. S.; Lee, T.; Geckeler, K. E. *Angew. Chem., Int. Ed.* **2006**, *45*, 104. (c) Zhang, R.; Wang, X. *Chem. Mater.* **2007**, *19*, 976.
- (9) Wang, D.; Li, Z. C.; Chen, L. *J. Am. Chem. Soc.* **2006**, *128*, 15078.
- (10) Tao, L.; Chen, G.; Mantovani, G.; York, S.; Haddleton, D. M. *Chem. Commun.* **2006**, 4949.
- (11) Richard, C.; Balavoine, F.; Schultz, P.; Ebbesen, T. W.; Mioskowski, C. *Science* **2003**, *300*, 775.
- (12) Belloni, J.; Mostafavi, M.; Remita, H.; Marignier, J. L.; Delcourt, M. O. *New J. Chem.* **1998**, *22*, 1239.
- (13) Zheng, H. T.; Li, Y.; Chen, S.; Shen, P. K. *J. Power Sources* **2006**, *163*, 371.

JA8026373